Central European Journal of Energetic Materials
ISSN 1733-7178; e-ISSN 2353-1843

Cent. Eur. J. Energ. Mater. 2018, *15*(2): 299-314; DOI: 10.22211/cejem/89866

Extrudable Gassy Pyrotechnic Time Delay Compositions

Johannes M. Grobler, Andrew W. Cowgill, Walter W. Focke,* George Labuschagne

Institute of Applied Materials, University of Pretoria, Private Bag X20, Hatfield, 0028 Pretoria, South Africa
**E-mail: Walter.Focke@up.ac.za*

Abstract: A copolymer of chlorotrifluoroethylene and vinylidene fluoride was investigated to assess its viability as an oxidiser, for aluminium as the fuel, in an extrudable pyrotechnic composition for application in 3D printing. Experimental results and EKVI thermochemical modelling suggested that a fuel loading of 30 wt.% would provide the maximum energy output. DTA and TGA analysis were performed in order to ascertain processing limits. With the addition of a processing aid LFC-1® samples could be extruded successfully. Printing with the compositions had limited success. The high melt viscosity paired with the filament's susceptibility to excessive preheating caused the print quality to be low. Delamination did not occur due to good fusion achieved during layer deposition. With minor compositional adjustments printing quality could be improvedy.

Keywords: polymer, burning rate, pyrotechnic, ignition time

1 Introduction

Traditional pyrotechnic compositions may contain undesirable heavy metals such as lead, mercury, barium, and cadmium [1-3]. These pose environmental concerns that mandate their replacement with more benign compounds [4]. Some pyrotechnic formulations contain chlorinated organic compounds (*e.g.* PVC) and/or mixtures of hydrocarbons and perchlorates. When these burn highly toxic compounds such as polychlorinated dibenzodioxins (PCDDs), polychlorinated dibenzofuranes (PCDFs) and polychlorinated biphenyls (PCBs) are potentially released [5]. Whether the amounts released actually pose a significant risk is being debated [6, 7]. However, the fact remains that such pyrotechnic devices

do release these polychlorinated compounds into the environment.

Pyrotechnic reactions can essentially be viewed as reduction-oxidation (redox) reactions [8]. Metals with high reducing potentials act as fuels when mixed with halogen-containing compounds, in particular those based on fluorine. The reaction is highly exothermic owing to the formation of very stable metal-halogen bonds (M–X). Fluorine is the preferred halogen above others such as chlorine as the heat of formation of the metal-fluorine bond is much higher [9]. Fluorinated polymers are also attractive alternatives for oxidisers such as the perchlorates. Fluorinated polymers are already used as oxidisers and also serve as binders for active compositions. Unfortunately, the most highly fluorinated polymer, PTFE, does not flow above its melting point and it is therefore not melt processable. However, copolymers of tetrafluoroethylene (TFE) and chlorotrifluoroethylene (CTFE) have lower melting points and are also soluble in common organic solvents [10, 11]. This facilitates processing and manufacture of corresponding pyrotechnic compositions using conventional polymer technologies such as extrusion as well as novel production procedures such as fused deposition modelling (FDM), a form of additive manufacturing [12]. However, some fluorine-based copolymers may contain vinylidene fluoride (VDF) or ethylene in their backbone structure. Unfortunately the presence of hydrogen may lead to the undesirable formation of hydrofluoric acid (HF) and/or hydrochloric acid (HCl) under burning conditions [13, 14].

This communication reports on a conceptual study that explored the use of an aluminium-filled fluoropolymer as an extrudable time-delay composition. Such a technology, if successful, could be used to mass produce open-burn fuses using conventional polymer technology. The extruded filaments could also be employed in 3D printing of energetic materials for purposes other than effecting time-delays.

2 Materials and Methods

2.1 Thermodynamic simulations

Thermodynamic simulations were performed using EKVI thermodynamic software. The adiabatic reaction temperatures, energy outputs and product spectra were predicted as a function of feed composition.

2.2 Materials

3M supplied the FK-800 resin, a copolymer of CTFE with 16 wt.% VDF, and also an oligomer grade of poly(vinylidenefluoride-co-hexafluoropropylene)

marketed under the trade name LFC-1. The former was the main oxidiser while the latter was used as an extrusion processing aid while simultaneously acting as a secondary oxidiser [9]. Aluminium powder was supplied by Grinman, South Africa. Magnesium powder was supplied by Merck. The Filament Factory supplied a reel of poly(lactic acid) filament designed for 3D printing according to the fused deposition modelling technology. This sample was used as rheology reference material. All materials were used as delivered but the aluminium powder was sieved through a 25 μm screen before use.

2.3 Characterization

Particle size analysis of the aluminium powder was performed using a Mastersizer Hydrosizer 2000 instrument with the powder dispersed in water. Surface area analysis was performed using a Micromeritics Tristar II BET surface and porosity analyser using liquid nitrogen and a nitrogen atmosphere.

TGA analysis was performed on a Hitachi STA7300 Thermal Analysis System. The samples were weighed and placed in alumina crucibles for analysis. Samples were heated at a scan rate of 10 °C·min^{-1} from ambient temperature to 600 °C. Runs were performed in a nitrogen atmosphere.

XRF measurements were performed using an ARL Perform'X Sequential XRF instrument and data analysis was done using Uniquant software. XRD diffractograms were obtained in a Bruker D8 Advance diffractometer with 2.2 kW Cu Kα radiation $\lambda = 1.5406$ nm fitted with a LynxEye detector with a 3.7° active area. Samples were scanned in reflection mode in the angular range 5° to 90° 2θ.

Scanning electron microscope (SEM) imaging was done on a ZEISS Gemini ULTRA Plus field emission scanning electron microscope at 1 kV. This revealed the morphology of the aluminium particles and the morphologies of the combustion residues recovered from the bomb calorimeter tests. Chemical identification of particular entities observed in the powder residues was done using the SEM-EDS option on the SEM together with AZtec software.

Rheology measurements were conducted at 230 °C on a SmartRheo capillary rheometer. The piston type 8.09 PT was used, the capillary diameter was 1 mm and the L/D ratio was 5.

2.4 Sample preparation

Pyrotechnic films were prepared using solvent casting. The polymer was dissolved in tetrahydrofuran (THF). Aluminium powder was added to make 2 g final composition. The mixture was left to stir until homogeneous and then emptied into a Teflon-coated tray and placed in a hood. The solvent was allowed to evaporate under ambient conditions. These samples were then used to measure

the heat of combustion with a bomb calorimeter.

Preliminary compounding and extrusion trials were conducted using an inert simulant instead of the aluminium fuel. This was done to establish safe processing procedures and to determine suitable operating windows for extrusion and 3D printing. Magnesium hydroxide was chosen instead of aluminium trihydrate because it is stable up to about 320 °C whereas the latter decomposes at about 210 °C. The magnesium hydroxide content was set at 27 wt.%. This level was selected as it corresponds to a similar volume fraction of filler as in the case for the 30 wt.% aluminium-filled FK-800 compound. The compounding trials with magnesium as fuel simulant were conducted on a TX28P co-rotating twin screw extruder with a barrel diameter of 28 mm and an L/D ratio of 18:1. The screw design comprised intermeshing kneader elements with a forward transport action. The screw speed was set to 20 rpm. The temperature profile, from hopper to die, was 190/210/220/230/230 °C. The extruded strand was cooled in a water bath and pelletized. These pellets were used for the rheology measurements.

The compounded pellets were also used to extrude filaments on a Filament Factory-built 18 mm ϕ laboratory-scale single screw extruder with an L/D ratio of 23:1. The temperature profile, from hopper to die, was 190/210/220/230 °C and the screw speed was set at 46 rpm. In this case the extruded filament was cooled using a water spray. A final filament diameter of 1.75 ± 0.10 mm was achieved by an integrated thickness controller utilising a laser micrometer. For compounding trials of the actual energetic compositions, the aluminium was first mixed with the fluoropolymer LFC-1. This was achieved by rolling the aluminium into the wax-like substance. This mixture was then granulated before blending with the main polymer and feeding it to the compounding extruder. The energetic compositions were compounded on a Thermo Scientific Process 11 co-rotating twin-screw compounding extruder. The screw speed was set at 320 rpm. The temperature profile along the extruder barrel, from hopper to die, was 140/170/180/190/200/210/220/230 °C.

2.5 Energetic testing

Bomb calorimetry was performed with a Parr 6200 calorimeter. The tests were carried out in a 3.0 MPa helium atmosphere. 500-700 mg of sample was weighed into the pan and ignited using an electrically heated 30 gauge nichrome wire.

Differential thermal analysis (DTA) runs were conducted on a Shimadzu DTA-50 Differential Thermal Analyzer. 10-15 mg sample was weighed into an alumina pan and an equal mass of DTA standard aluminium oxide (Al_2O_3) was weighed into the reference pan. The temperature was scanned from 30 °C to

600 °C at a rate of 50 °C·min^{-1} in order to determine the ignition temperature of the compositions.

Burn rate measurements were performed on extruded filaments. Samples were placed in a 2 mm deep and 4 mm wide groove cut into a pyrophyllite block. The samples were partially covered by an alumina tile. The samples were cut to be 10.5 cm long with the last 5.7 cm of the sample being used as the measurement zone. This zone was monitored by a PYROVIEW 380L compact infrared camera. The filament samples were ignited by contact with a butane torch. The recorded IR data was analysed using Pyrosoft Professional version 2.15.1 software. The combustion temperature was measured during these tests using a Raytek pyrometer.

Ignition tests were done utilising the same IR camera and software. The samples were ignited with a Synrad model 48-2 carbon dioxide laser with wavelength of 10.6 μm. The beam diameter was 1.72 mm. Ignition tests were done in a power range between 2 W and 10 W.

2.6 Printing trials

Fused deposition modelling (FDM) printing trials were performed using a modified E3D V6 direct feed hot end with a nozzle diameter of 1.2 mm. The hot end was designed for a filament diameter of 1.75 mm. The hot end was mounted on a Printrbot Simple model 1403 printer. The printing temperature was 230 °C and a heated bed was used to assist with the adhesion of the printed part.

3 Results

3.1 Characterization

The aluminium powder was found to be X-ray pure. A representative SEM image showing the morphology of the particles is shown in Figure 1. The particles had a BET surface area of 2.4 m^2·g^{-1} and a median particle size (d_{50}) of 10.7 μm. Particle size analysis indicated that approximately 12 vol.% of the particles were larger than 25 μm.

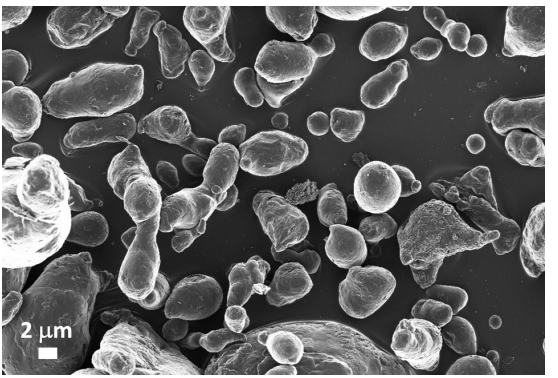

Figure 1. SEM image of aluminium particles used as fuel

TGA analysis was performed in order to establish the temperature at which mass loss commenced in the polymers. This information provided a first indication of the maximum allowable processing temperatures that could be considered. According to Figure 2, the mass loss onset temperatures were 360 °C and 244 °C for FK-800 and LFC-1, respectively.

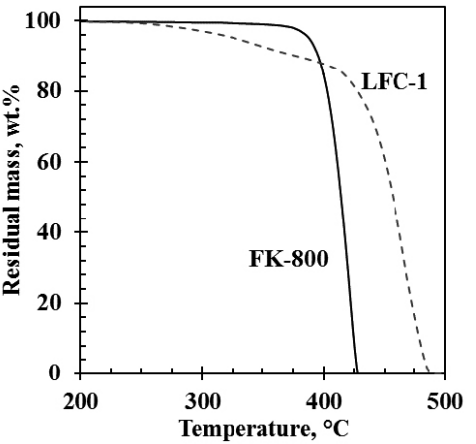

Figure 2. TGA analysis of FK-800 (poly(chlorotrifluoroethylene-co-vinylidene fluoride)) and LFC-1 (poly(vinylidenefluoride-co-hexafluoropropylene)) in a nitrogen atmosphere

3.2 Extrusion and rheology

The fluoropolymer FK-800 was successfully extruded into a filament and showed minimal signs of thermal degradation. In order to assess the impact

of adding a solid filler on the mechanical properties and the extrudability of the polymer, magnesium hydroxide was used as inactive simulant in place of the aluminium fuel. A filament of FK-800 containing 27 wt.% $Mg(OH)_2$ was successfully compounded and converted into filament. Addition of the LFC-1 visibly improved the processability by lowering the melt viscosity and yielding a smoother surface texture of the extrudate.

Figure 3 shows the melt viscosity curves for three compounds. At the lower shear rates, relevant to FDM, the neat FK-800 resin exhibits a melt viscosity that is similar or lower than the PLA resin tailor-made for FDM. Inclusion of the magnesium filler significantly raised the melt viscosity. A similar viscosity increase was expected for the aluminium-filled energetic material.

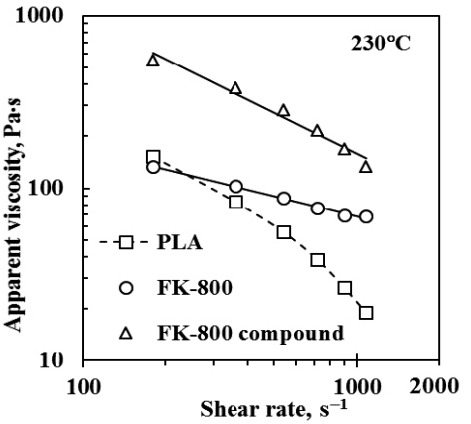

Figure 3. Capillary rheometer melt viscosity *vs*. shear rate curves for neat FK-800 as well as a compound containing 27 wt.% magnesium hydroxide. The viscosity curve for the PLA grade used for 3D printing is included as a reference

3.3 Thermochemical simulation

Figure 4 shows the adiabatic reaction temperature profile for the reaction of aluminium fuel with the main oxidiser. The simulation was conducted for open burn conditions, *i.e*. constant 1 atm pressure and allowing free expansion of any product gases. The predicted maximum adiabatic reaction temperature was 2972 °C at an aluminium fuel loading of 23 wt.%.

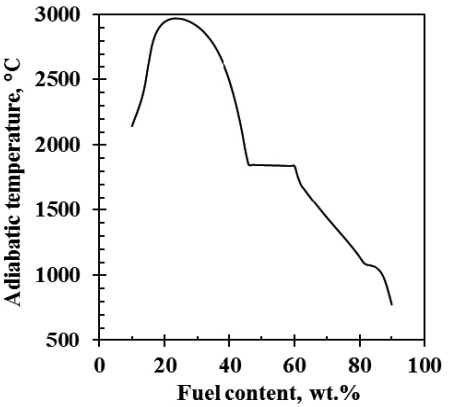

Figure 4. EKVI simulation of the combustion reaction between aluminium as fuel and a combination of chlorotrifluoroethylene (84 wt.%) and vinylidene fluoride (16 wt.%) as an oxidiser, at a fixed pressure of 1 atm

EKVI simulations were also performed for the conditions expected in the bomb calorimeter detailed above, *i.e.* 240 mL volume, 30 MPa initial helium atmosphere. The simulated energy output as a function of fuel loading is shown in Figure 5. The maximum energy output predicted for the compositions was 7.52 $MJ \cdot kg^{-1}$ at a fuel loading of 23 wt.%.

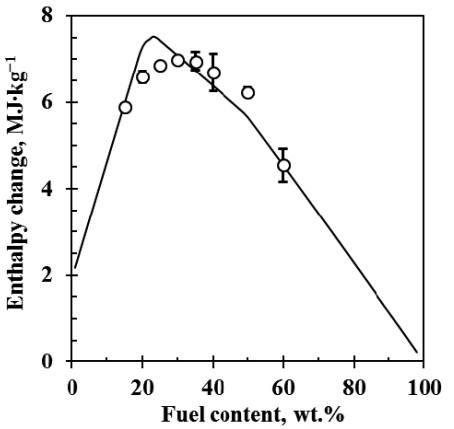

Figure 5. EKVI-predicted (solid curve) enthalpy changes, simulated under bomb calorimeter conditions of 30 MPa He atmosphere, compared to experimental results. The combustion reaction was for aluminium as fuel and a mixture of vinylidene fluoride (16 wt.%) and chlorotrifluoroethylene (84 wt.%) as the oxidisers

It must be noted that the database used by the software did not cater for polymers. Therefore, the reported results did not take into account the enthalpy of polymerisation of the monomers into the polymer. Instead, the reactions were simulated with the correct molar ratios of the monomer gases. In the bomb calorimeter, gas production is suppressed due to the high pressure helium atmosphere. Thus in an open burn, where gas production is not limited, much of the energy produced was consumed by the vaporisation of products instead of increasing the sensible heat (*i.e*. raising the temperature) of the reaction products.

3.4 Energetic tests

Bomb calorimeter results for films consisting of various fuel loadings are also shown in Figure 5. The maximum energy output from the bomb calorimeter was 7.0 $MJ \cdot kg^{-1}$ and occurred at a fuel loading of 30 wt.%. The discrepancy between the simulated and experimental results can be explained by the fact that the simulation assumed complete reaction which, in reality, is not the case. Also, the enthalpy of polymerisation was not taken into account as explained above. Nevertheless, the experimental results approximately matched the simulated values.

All compositions ignited successfully, however, the 15 wt.% composition misfired on one attempt and needed to be re-prepared. When the bomb was opened, the composition showed signs of charring where the nichrome wire had been in contact with the composition during the attempted ignition. This indicated that a composition of approximately 15 wt.% fuel is approaching the lower limit for successful burning. Overall the composition is very insensitive to ignition and with a lower fuel content did not ignite at all. However, the 15 wt.% composition did ignite successfully on a subsequent attempts.

3.5 Ignition tests

The ignition temperature is an important consideration when designing a system intended for extrusion. Due to the high viscosity of polymer melts, there is a significant amount of viscous heating that takes place inside extruders. The temperature profiles presented by Kelly *et al*. [15] demonstrate this fact, with the temperature at the centre of the polymer flow being up to 30 °C hotter than at the wall. Beyond the polymer compound rheology, this temperature differential is affected by variables such as the barrel temperature profile, screw speed, screw and die geometry, *etc*.

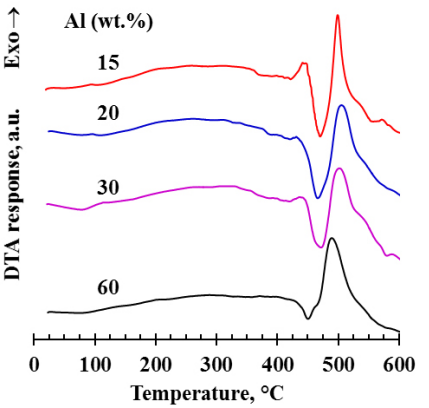

Figure 6. DTA response curves for FK-800 at various aluminium fuel loadings

Figure 6 shows the DTA-determined ignition temperatures of the FK-800 system. The ignition temperatures were found to be nearly independent of the fuel loading. They ranged between 460 °C and 470 °C across the composition range tested. This suggests that the reaction was dependent on the degradation of the oxidiser as these temperatures were too low for the aluminium to undergo any phase change.

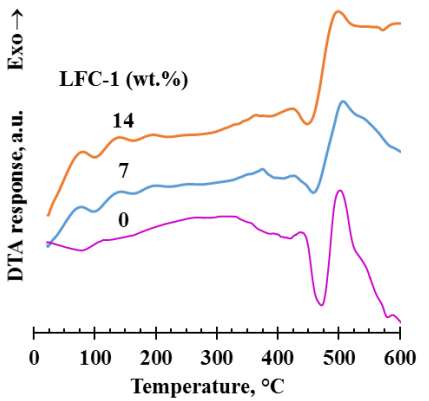

Figure 7. DTA response curves for compositions containing 30 wt.% aluminium fuel with partial substitution of the FK-800 oxidant with various amounts of LFC-1

Addition of LFC-1 caused a slight shift in the ignition temperature for the 30 wt.% aluminium system. This is illustrated in Figure 7 which shows

a reduction of the ignition temperature to 450 °C for the 14 wt.% LFC-1 loading. LFC-1 probably decomposes at a lower temperature releasing the oxidizing components faster than the main oxidizer thereby sensitizing the system. These observations support the hypothesis that the ignition mechanism is a gas-solid reaction.

The recommended processing temperature for FK-800 is approximately 230 °C. The experimentally-determined ignition temperatures are therefore more than 200 °C higher than the recommended processing temperature. This means that these compositions should be sufficiently thermally stable to allow safe compounding and extrusion.

3.6 Burn rate and time to ignition

The measured burning rate results, listed in Table 1, were comparable to results obtained in other studies [12, 16]. Filaments extruded for 3D printable compositions based on PVDF, with 20 wt.% aluminium as fuel, exhibited burning rates of up to 18.7 ±1.3 mm·s^{-1} [12]. Potgieter *et al.* [16] measured the burning rates of energetic films based on Viton B fluoropolymer as oxidant with 50 wt.% metal fuel. Their films had a thickness of 245 ± 21 μm and they were prepared *via* a slurry casting process. Burning rates of 82 mm·s^{-1} and 40 mm·s^{-1} were achieved with magnalium and flake aluminium as fuels, respectively.

Table 1. Burn rates and temperatures measured for FK-800 compositions containing 30 wt.% aluminium fuel

LFC-1 loading [wt.%]	7	14
Burn temperature [°C]	794	971
Burn rate [mm·s^{-1}]	15.9 ±2.2	18.9 ±4.6

The processing aid, LFC-1, had a significant impact on the combustion performance of the system. As its loading increased to 14 wt.%, higher reaction temperatures were noted. The burn rate became faster but at the cost of reproducibility. The variance for the burn rate doubled with the increased LFC-1 content. The variability of the burn rate provides an indication of the quality of the extruded filaments [12]. The burn rate increases can be explained by the increase in the reaction temperature.

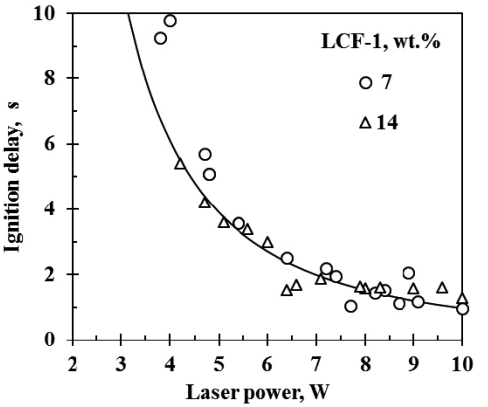

Figure 8. Results of laser ignition studies for the two LFC-1 loadings

Time to ignition studies were performed using laser ignition and the results are reported in Figure 8. The ignition time (t_{ign}) is dependent on various factors including ignition temperature (T_{ign}), starting temperature (T_0), power flux (q), thermal conductivity (k) and thermal diffusivity (α). An elementary expression that captures these functional dependencies, and derived on the basis of several simplifying assumptions, is shown in Equation 1 below [17]:

$$t_{ign} = \frac{\pi}{4\alpha q^2}\left[k\left(T_{ign} - T_0\right)\right]^2 \quad (1)$$

Higher LFC-1 concentrations decreased the time to ignition in DTA studies. However, the scatter in the laser ignition data was such that no difference could be discerned with any confidence.

3.7 Residue analysis

The solid products were collected from the bomb calorimeter after burning. The combustion products appeared black except that at higher fuel loadings there were some yellow particles scattered throughout the residue. Figure 9 shows SEM images of the residues. The primary products appeared to be the cubic crystals shown in Figures 9a and 9b along with the much smaller nano-sized particles covering the larger crystals. These cubes and nanoparticles were present in the residues from all compositions. SEM-EDS analysis indicated that these were aluminium fluoride (AlF_3) and carbon respectively. As the fuel loading increased, much larger spherical residues were observed as in Figure 9c. The higher the fuel loading, the more of these spherical particles were observed. It was initially thought that these particles were unreacted aluminium particles, however, further analysis

proved them to be AlF_3 as well. At very high fuel loadings hexagonal crystals, as shown in Figure 9d, were noticed in the residues. These crystals were aluminium carbide (AlC) crystals which are naturally hexagonal [18]. AlC decomposes on contact with moisture to release methane. This explains the foul odour noticed on opening the bomb after the high fuel-content compositions were burned. It also explains the yellow colour of the particles, as AlC is yellow. In accord with the predictions of the EKVI simulations, the formation of AlC only occurred at fuel loadings above 25 wt.% and increased to a maximum at a fuel loading of 60 wt.%. This explains why these crystals were only noticed at very high fuel loadings.

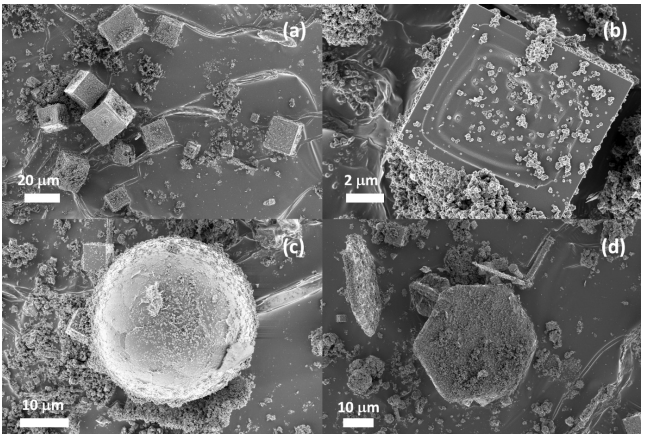

Figure 9. SEM micrographs of burn residue for compositions with aluminium fuel loadings of (a) and (b) 20 wt.% (c) 40 wt.% (d) 60 wt.%

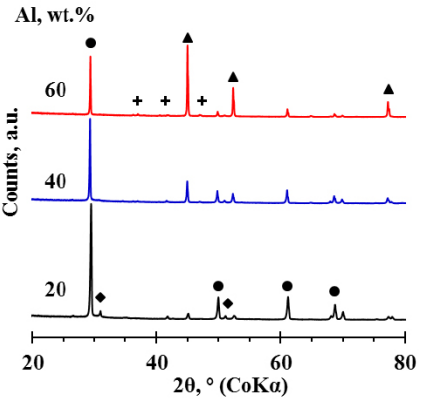

Figure 10. XRD diffractograms for reaction residues at various fuel loadings. Reflections indicate the following phases: ● − aluminium fluoride; ▲ − aluminium; ◆ − graphite, ✚ − aluminium carbide

XRD analysis results of the residues are presented in Figure 10. These results confirm that the formation of AlF_3 and graphite decreased with an increase in fuel loading. Similarly, the AlC and unreacted aluminium fractions increased with an increase in fuel loading.

3.8 Printing trials

Initial printing trials highlighted several issues, the first being the relatively high viscosity of the polymer melt. The printing temperature could not be adjusted to rectify this as the printing temperature was already approaching the processing temperature limit indicated by the supplier. At the temperature used, the filament was experiencing excessive heating above the heating block. This heat was conducted back causing softening and swelling in the feeding tube leading to the heating block. This premature melting of the polymer was due to the high thermal conductivity imparted by the high aluminium content of the filament. This conclusion was informed by the fact that a similar problem did not occur when the aluminium filler present in the filament was replaced by a corresponding volume fraction magnesium hydroxide. Several adjustments were implemented in order to obtain a successful print run with the composition in question. A change to a larger diameter nozzle was made in order to reduce the pressure required to force the melt out of the extruder. Acceptable flow was achieved by increasing the nozzle diameter from the original diameter of 0.4 mm to 1.2 mm. Also, the feeder tube was enlarged to 2.4 mm to accommodate the swelling of the filament. Even with these modifications, feeding was still problematic. The high viscosity of the melt meant that there was a high resistance to flow and this increased the printing time. The side view of a printed rectangle shown in Figure 11, also reveals that the print quality was not of a high standard.

Figure 11. Side-on view of a 3D fused deposition printed track

The feeding issues discussed caused inconsistent polymer flow which led to the bulging sections in Figure 11. Even with these obvious defects the individual layers were fused and delamination was not an issue for the small

parts printed. This shows that with further improvement of the formulation, *e.g.* using lower molar mass fluoropolymers with a lower melt viscosity, 3D printing may become a viable option. Another option that could be explored would be to lower the aluminium content of the composition. The mass loading of 30 wt.% was selected as the initial analysis indicated it to be the one providing the most intense energetic performance. This may however be too high a loading for higher quality printing as the metal filler increases the viscosity and thermal conductivity of the composition.

4 Conclusions

A melt processable composition consisting of 30 wt.% aluminium fuel incorporated into poly(chlorotrifluoroethylene-co-polyvinylidene fluoride) as main oxidant together with a processing aid represented by a waxy oligomer of poly(vinylidenefluoride-co-hexafluoropropylene) was formulated. Melt compounding and extrusion of constant thickness filaments of this composition was facile. These filaments burned at rates of 16 mm·s^{-1} to 19 mm·s^{-1}, depending on the processing aid content. However, 3D printing by fused deposition modelling was complicated by the high viscosity of the melt and axial heat conduction. The processing aid was unable to decrease the melt viscosity sufficiently even at a loading of 14 wt.%. Its inclusion decreased the time to ignition and increased both the burn rate and burn temperature.

Acknowledgements
The authors gratefully acknowledge financial and technical support from AEL Mining Services. Financial support from the THRIP program of the Department of Trade and Industry and the National Research Foundation is also gratefully acknowledged.

References

[1] Danali, S.; Palaiah, R.; Raha, K. Developments in Pyrotechnics. *Def. Sci. J.* **2010**, *60*(2): 152-158.
[2] Ilyushin, M. A.; Tselinsky, I. V.; Shugalei, I. V. Environmentally Friendly Energetic Materials for Initiation Devices. *Cent. Eur. J. Energ. Mater.* **2012**, *9*(4): 293-327.
[3] Steinhauser, G.; Klapötke, T. M. "Green" Pyrotechnics: A Chemists' Challenge. *Angew. Chem., Int. Ed.* **2008**, *47*(18): 3330-3347.

[4] Fronabarger, J. W.; Williams, M. D.; Sanborn, W. B.; Bragg, J. G.; Parrish, D. A.; Bichay, M. DBX-1 – A Lead Free Replacement for Lead Azide. *Propellants Explos. Pyrotech.* **2011**, *36*(6): 541-550.
[5] Sabatini, J. J., Koch, E.-C.; Poret, J. C.; Moretti, J. D.; Harbol, S. M. Chlorine-Free Red-Burning Pyrotechnics. *Angew. Chem., Int. Ed.* **2015**, *54*(37): 10968-10970.
[6] Fleischer, O.; Wichmann, H.; Lorenz, W. Release of Polychlorinated Dibenzo-p-dioxins and Dibenzofurans by Setting Off Fireworks. *Chemosphere* **1999**, *39*(6): 925-932.
[7] Dyke, P.; Coleman, P.; James, R. Dioxins in Ambient Air, Bonfire Night 1994. *Chemosphere* **1997**, *34*(5): 1191-1201.
[8] Steinhauser, G.; Klapötke, T. M. Using the Chemistry of Fireworks to Engage Students in Learning Basic Chemical Principles: A Lesson in Eco-friendly Pyrotechnics. *J. Chem. Educ*. **2010**, *87*(2): 150-156.
[9] Koch, E.-C. *Metal-Fluorocarbon Based Energetic Materials*. Wiley VCH, Weinheim **2012**; ISBN 9783527329205.
[10] Fleck, T. J.; Murray, A. K.; Gunduz, I. E.; Son, S. F.; Chiu, G. T.-C.; Rhoads, J. F. Additive Manufacturing of Multifunctional Reactive Materials. *Additive Manuf.* **2017**, *17*: 176-182.
[11] Huang, C.; Yang, H.; Li, Y.; Cheng, Y. Characterization of Aluminum/Poly(Vinylidene Fluoride) by Thermogravimetric Analysis, Differential Scanning Calorimetry, and Mass Spectrometry. *Anal. Lett.* **2015**, *48*(13): 2011-2021.
[12] McCollum, J.; Pantoya, M. L.; Iacono, S. T. Activating Aluminum Reactivity with Fluoropolymer Coatings for Improved Energetic Composite Combustion. *ACS Appl. Mater. Interfaces* **2015**, *7*(33): 18742-18749.
[13] Boschet, F.; Ameduri, B. (Co)polymers of Chlorotrifluoroethylene: Synthesis, Properties, and Applications. *Chem. Rev.* **2013**, *114*(2): 927-980.
[14] Martinez, H.; Zheng, Z.; Dolbier, W. R. Jr. Energetic Materials Containing Fluorine. Design, Synthesis and Testing of Furazan-Containing Energetic Materials Bearing a Pentafluorosulfanyl Group. *J. Fluorine Chem.* **2012**, *143*: 112-122.
[15] Kelly, A. L.; Brown, E. C.; Coates, P. D. The Effect of Screw Geometry on Melt Temperature Profile in Single Screw Extrusion. *Polym. Eng. Sci.* **2006**, *46*(12): 1706-1714.
[16] Potgieter, G.; Focke, W. W.; Labuschagné, G. D.; Kelly, C. Fluoroelastomer Pyrotechnic Time Delay Compositions. *J. Thermal Anal. Calorim.* **2016**, *126*(3): 1363-1370.